CHEMMEDCHEM

CHEMISTRY ENABLING DRUG DISCOVERY

Accepted Article

Title: Structure-Activity Relationship of Propargylamine-Based HDAC Inhibitors

Authors: Matthias Wünsch, Johanna Senger, Philipp Schultheisz, Sabrina Schwarzbich, Karin Schmidtkunz, Carmela Michalek, Michaela Klaß, Stefanie Goskowitz, Philipp Borchert, Lucas Praetorius, Wolfgang Sippl, Manfred Jung, and Norbert Sewald

To be cited as: *ChemMedChem* 10.1002/cmdc.201700550

Link to VoR: http://dx.doi.org/10.1002/cmdc.201700550

A Journal of

ChemPubSoc Europe

WILEY-VCH

www.chemmedchem.org

Structure-Activity Relationship of Propargylamine-Based HDAC Inhibitors

Matthias Wünsch[a], Johanna Senger[b], Philipp Schultheisz[a], Sabrina Schwarzbich[a], Karin Schmidtkunz[b], Carmela Michalek[a], Michaela Klaß[a], Stefanie Goskowitz[a], Philipp Borchert[a], Lucas Praetorius[c], Wolfgang Sippl[c], Manfred Jung[b], Norbert Sewald[a],*.

[a] M. Wünsch (ORCID 0000-0002-3244-8374), P. Schultheisz, S. Schwarzbich, C. Michalek, M. Klaß, S. Goskowitz, P. Borchert, Prof. Dr. N. Sewald (ORCID 0000-0002-0309-2655)
Organic and Bioorganic Chemistry
Bielefeld University
Universitätsstrasse 25, 33615 Bielefeld, Germany
Norbert.Sewald@uni-bielefeld.de

[b] Dr. J. Senger, K. Schmidtkunz, Prof. Dr. M. Jung (ORCID 0000-0002-6361-7716)
Institute of Pharmaceutical Sciences
Albert-Ludwigs-Universität Freiburg
Albertstrasse 25, 79104 Freiburg im Breisgau, Germany

[c] L. Praetorius, Prof. Dr. W. Sippl (ORCID 0000-0002-5985-9261)
Institute of Pharmacy
Martin-Luther-Universität Halle-Wittenberg
Wolfgang-Langenbeck-Str. 4, 06120 Halle/Saale, Germany

Supporting information for this article is given via a link at the end of the document.

Abstract: As histone deacetylases (HDACs) play an important role in cancer treatment, their selective inhibition has been subject of various studies. The continuous investigations have spawned a large collection of pan- and selective HDAC inhibitors, containing diverse FDA approved representatives. In former studies, a class of alkyne based inhibitors of HDACs was presented. We modified this scaffold in two previously neglected regions and compared cytotoxicity and affinity towards HDAC1, HDAC6 and HDAC8. We could show that (*R*)-configured propargylamines contribute increased selectivity on HDAC6, while the size of the substituents decreases their affinity. Docking studies on available HDAC crystal structures were carried out to rationalize the observed selectivity of the compounds. Substitution of the aromatic part by a thiophene derivative results in high affinity and low cytotoxicity, indicating an improved drug tolerance.

Introduction

Controlling diverse cellular functions by deactivating transcription makes histone deacetylases important effector molecules for epigenetic regulation and also a therapeutic target. They are divided into four classes according to their function, localization and sequence homology.[1] The inhibition of certain HDACs is an approach for versatile pharmaceutical applications like the regulation of autoimmunity,[2] influence on neurological processes [3] or suppression of tumor growth.[4–6] The development of non-selective HDACis (Figure 1) including Vorinostat (SAHA),[7] Trichostatin A,[8] Belinostat,[9] Panobinostat,[10] Oxamflatin,[11] Tubastatin A [12] and Romidepsin (depsipeptide FK228) [13] has already proceeded very far and some have even been clinically established (Vorinostat, Belinostat, Panobinostat, Romidepsin and Tucidinostat).[7,14] The benzamide Tucidinostat has achieved particular relevance in clinical studies, as it is selective on HDAC 1, 2, 3 and 10.[15]

However, the inhibition of class I and class IIA HDACs may lead to serious side effects that have not been reported for class IIB, class III, and IV HDACs. For example HDAC1 knockout leads to embryonic lethality [16] and HDAC2, -5, and -9 knockouts provoke cardiac defects.[17,18] HDAC6 selective inhibitors do neither show a change in gene expression in microarray analysis,[19] nor do KO mice show abnormal development or problems with organ functions.[20] In addition to the modulation of transcription, HDAC6 uniquely deacetylates α-tubulin,[21] decreasing the speed of vesicle transport, what makes selective inhibitors of HDAC6 a promising drug candidates against neurodegenerative diseases like for example Huntington's disease.[22–24]

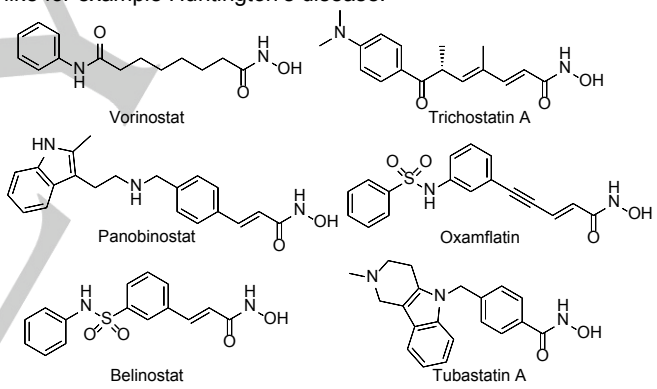

Figure 1. Chemical structures of a selection of important HDAC inhibitors.[7,14]

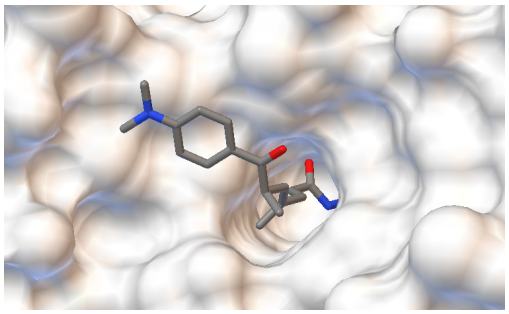

Figure 2. X-ray structure analysis of the active site of HDAC6 occupied by Trichostatin A (TSA).[25]

The active sites of HDAC1, 6, and 8 consist of a hydrophobic channel that is terminated by a bound Zn^{2+} ion, which catalyzes deacetylation of lysine residues.[26–28] The active site structure of

HDAC6 has been recently elucidated (Figure 2),[25,29] allowing accurate design of inhibitor topology.
Potent inhibitors consist of a Zn^{2+} binding group like a ketone, benzamide, carboxylic acid, or hydroxamic acid at one end that is terminated by an inflexible, rod-like linker with a cap group at the other end.[30,31] Sendzik et al. proposed an achiral propargylamine scaffold for a new generation of HDAC inhibitors and modified the cap group (Figure 3), which is the most promising part to induce selectivity.[32]

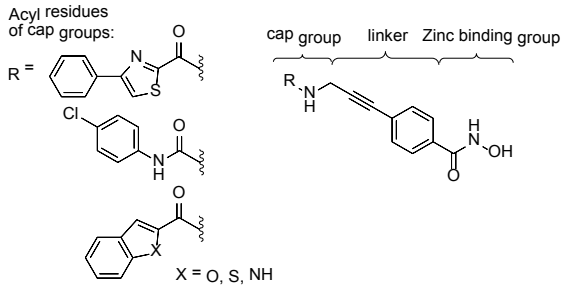

Figure 3. Canonical structures of potent HDAC inhibitors based on an achiral propargylamine with different cap groups at the *N*-terminus.[32]

We became interested in the influence of chirality in the propargylic position and introduced different linker regions with respect to the aromatic moiety, the configuration and size of the substituents.

Results and Discussion

We synthesized an array of potential HDAC inhibitors by combining different propargylamines linking the benzofuran cap group with aromatic hydroxamic acids.
The cap group of HDAC inhibitors is considered as the most important moiety to enhance selectivity and activity and has, therefore, been varied extensively.[32] Compounds **6a-g** vary with respect of configuration and size of the linker region and **6i** slightly deviates from linearity by incorporation of a five-membered heteroaromatic compound (Figure 4).
The distance between the hydroxamic acid and the propargylic position of our scaffold is almost equal to the length of the regular substrate of HDACs, the lysine side chain. That makes chiral analogues of other propargylamines with hydrophobic substituents promising alternatives. Combining three separately variable building blocks by click-reactions (as defined by Sharpless),[33] a large diversity of inhibitors can easily be achieved.
The building blocks of the linker regions are obtained by a convergent synthesis, linking an enantiopure propargylamine to a halogenated benzoic acid derivative in a Sonogashira cross-coupling (Table 1). Variations of the configuration and size of the substituent in propargylic position can be introduced by the application of substituted propargylamines.[34] The angle of the rigid linker can be modified by the use of heteroaromatic moieties (ar) like thiophene derivatives to 156°.
The propargylamines **4** are easily prepared by diastereoselective nucleophilic addition of trimethylsilylethynyl lithium to *N*-sulfinylimines. The *N*-sulfinyl group serves as the chiral auxiliary in the propargylamine preparation, as *S*-configured *N*-sulfinylimines direct the alkyne addition from the *re*-face, while *R*-configured *N*-sulfinylimines induce *si*-face additions.[35] Therefore, the *N*-sulfinyl propargylamines are either *R*,*R* or *S*,*S*-configured.[34] A diastereomeric excess of more than 99% is obtained, no other diastereomer was detected by ^{1}H NMR spectroscopy.
After cleavage of the sulfinamide, the terminal propargylamine is linked to a benzofuranoyl cap group according to Sendzik et al.[32] The aromatic methyl ester is finally converted to the zinc complexing hydroxamic acid by reaction of the methyl ester with hydroxylamine.
For the Sonogashira cross-coupling 1.6 equivalents of the aromatic halide were applied in order to achieve full conversion of the precious enantiomerically pure propargylamines. The products were formed in a mixture of THF/piperidine (3:1) in the presence of CuI (2%) and $Cl_2Pd(PPh_3)_2$ (1%) as catalyst. The application of pyridine, DIPEA, or 2,4,6-collidine or the application of $Pd(Ph_3)_4$ lead to a reduced yield. The progress of the reaction can be monitored by the precipitation of piperidinium iodide, which forms as a byproduct. Aqueous workup and purification by column chromatography provides the linker scaffolds **5a-h** in good yields (Table 1). Due to the strict exclusion of oxygen and the excess of aromatic halide, the commonly reported Glaser homocoupling under Sonogashira conditions can be excluded, as proven by mass spectrometry.

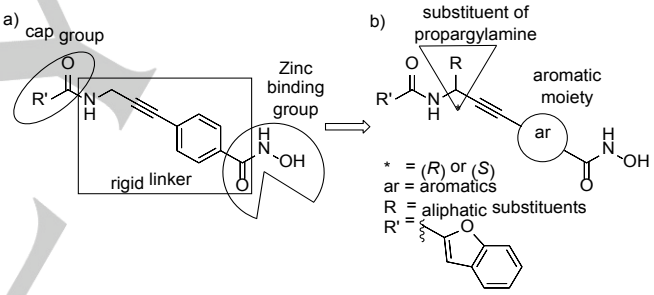

Figure 4. Design of inhibitors. a) Patent-registered inhibitor scaffold, used as model compound with extensively varied cap groups.[32] b) Variations of the model compound investigated in this work.

The Sonogashira cross-coupling of the heteroaromatic building blocks proceeds much more slowly and in lower yields, because halides **2b** and **2c** were only available as bromides instead of iodides. Furthermore, heteroaromatics like thiophene or pyridine are suspected to coordinate and poison the catalyst. In an effort to shorten the synthesis, methyl bromothiophene carboxylate **2c** was converted with aqueous hydroxylamine into hydroxamic acid derivative **3**. Dilution of the reaction mixture with cold Et_2O leads to precipitation of hydroxamic acid **3** in pure form. However, 5-bromothiophene-2-hydroxamate **3** did not react at all under Sonogashira cross-coupling conditions.
The corresponding amines are readily formed by acidic methanolysis of the sulfinamides **5a-i**. Water has to be excluded to avoid formation of *tert*-butylsulfinic acid. The methylsulfinate can be co-evaporated with DCM to quantitatively yield the amine hydrochlorides. The free amines can be converted without further purification with 2-benzofuranoyl chloride in dry DCM under basic conditions.

The hydroxamic acids **6** are obtained by reaction of the ester with an excess of aqueous hydroxylamine (50%). The reaction was monitored by mass spectrometry, which also showed formation of the acid as by-product. After aqueous workup and precipitation, the crude product was purified by preparative RP-HPLC. The low solubility in water, acetonitrile or any solvent (except for DMSO) leads to significant losses during purification.

The inhibitory activity of the synthesized compounds was determined (Table 1) in an assay developed by Schwienhorst et al.,[36,37] using a fluorescent substrate, invented by Jung et al.,[38] which is only cleaved in the enzymatic detection step when deacetylated. The HDAC activity depending on inhibitor concentration can be quickly determined by quantification of the fluorescence, caused by the released aminomethylcoumarin.[36,37]

Table 1. Synthesis of the inhibitor scaffolds upon reaction of enantiopure propargylamines with aromatic halides under Sonogashira cross-coupling conditions, acylation with the cap group and transformation of the methyl ester into a hydroxamic acid. Reaction conditions (a): $PdCl_2(PPh_3)_2$ (1%), CuI (2%), piperidine/THF (1:3), rt, 2-12 h. (b): 1) HCl (4 M in dioxane, 4 eq). 2) 2-benzofuranoyl chloride (1.5 eq), NEt_3 (6 eq), DCM, 0 °C, 6-14 h. 3) H_2NOH/H_2O/MeOH/THF (1:1:4:4), NaOH (pH = 10-11), rt, 16 h.

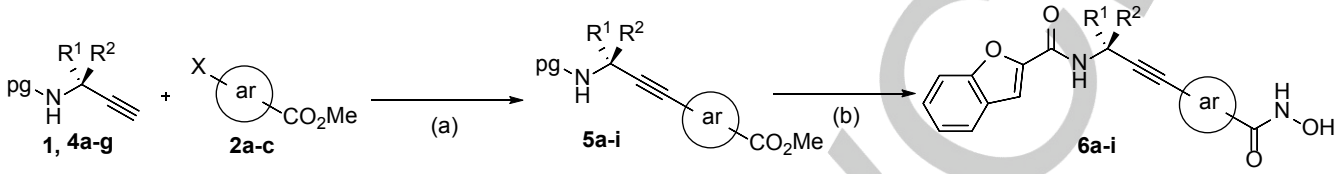

entry	pg	Propargyl-amine	R^1	R^2	Ar-X	**5**, yield	**6**, yield
a)	 (*S*)-Bus	**4a**	H	Cyclohexyl	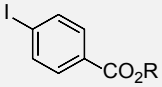 **2a** R = Me, Et	**5a**, 66%	**6a**, 24%
b)		**4b**	H	CH_2CHMe_2		**5b**, 94%	**6b**, 43%
c)		**4c**	H	$CHMe_2$		**5c**, 83%	**6c**, 16%
d) [a]	Boc	**1**	H	H		**5d**, 58%	**6d**, 3%
e)		**4e**	$CHMe_2$	H		**5e**, 64%	**6e**, 37%
f)		**4f**	CH_2CHMe_2	H		**5f**, 95%	**6f**, 9%
g)		**4g**	Cyclohexyl	H		**5g**, 74%	**6g**, 6%
h)	 (*R*)-Bus	**4g**	Cyclohexyl	H	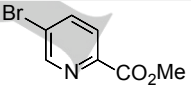 **2b**	**5h**, 41%	**6h**, 25%
i)		**4g**	Cyclohexyl	H	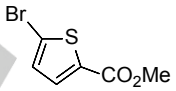 **2c**	**5i**, 23%	**6i**, 16%

[a] The synthesis of **6d**, entry d) had already been established by Sendzik et al.[32] and serves in this work as reference compound.

Table 2. Cytotoxicity and affinity of compounds **6a-i** to HDAC1, HDAC6, and HDAC8.

	HDAC1 [a] IC_{50} ± SEM [nM]	HDAC6 [a] IC_{50} ± SEM [nM]	Selectivity HDAC1/ HDAC6	HDAC8 [a] IC_{50} ± SEM [nM]	Selectivity HDAC8/ HDAC6	Cytotoxicity EC_{50} [µM] [b]
6a	161.5±30.6	119.4 ± 30.4	1.35	2200 ± 300	18.4	29±1.3
6b	80.2±10.2	64.4 ± 6.7	1.25	803 ± 111	12.5	13±0.2
6c	89.3±14.6	59.2 ± 9.2	1.51	916 ± 93	15.5	8.2±0.4
6d [c]	19.6±1.4	37.9 ± 4.1	0.52	232 ± 22	6.1	1.08±0.3
6e	127.9±19.3	15.6 ± 0.9	8.20	417 ± 53	26.7	4±0.7
6f	190.9±30.5	21.8 ± 1.6	7.40	862 ± 107	39.5	7.4±1.5
6g	268.5±95.3	25.3 ± 5.1	8.76	876 ± 125	34.6	29
6h	1150±150	72.1 ± 15.2	16.00	3300 ±400	45.8	100
6i	137.8±26.2	11.2 ± 1.1	12.30	1600 ± 200	142.9	44

[a] The affinity values were determined in an assay developed by Schwienhorst et al.[36,37] using a fluorescent substrate, invented by Jung et al.,[37] which is only cleaved enzymatically when deacetylated. The values of each inhibitor concentration were determined as triplicates for HDAC1 and HDAC6 and as technical and biological duplicates for HDAC8.
[b] Cytotoxicity values refer to cell line KB-3-1[40] and were determined as sixfold replicates for **6a-f** (± SEM) and as triplicates for **6g-h**.
[c] Compound **6d** published by Sendzik et al.[32] is used as reference compound.

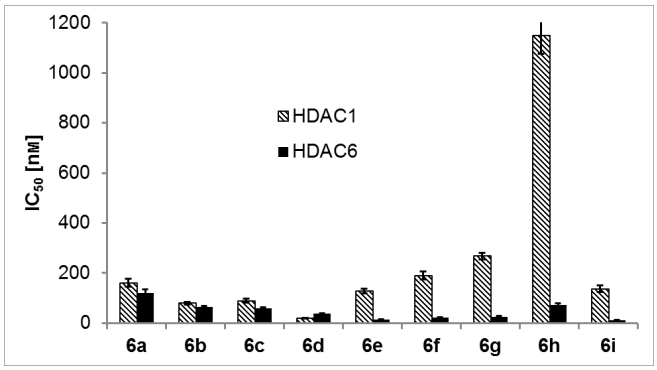

Figure 5. Inhibition (IC_{50} ± SEM) of HDAC1 and HDAC6 by compounds **6a-i**.

In comparison to HDAC6, the inhibition of HDAC8 by the hydroxamic acids **6a-i** is generally weaker with IC_{50} values in the range of 0.4-3.3 µM (6-142 times higher than for HDAC6).
The *S*-configured compounds **6a-c** are generally not very active against the HDAC tested, while potency towards HDAC6 decreases with increasing the size of the substituent in propargylic position. The *R*-configured compounds **6e-i** are potent inhibitors

of HDAC6 without significant influence of the substituent size R^1. However, selectivity towards HDAC6 is largely enhanced for *R*-configured compounds **6e-i** in comparison to the achiral parent compound **6d**, that even has a higher affinity to HDAC1 (Figure 5, Table 2).

As shown by X-ray structure analysis of the complex of HDAC6 and its inhibitor TSA (Figure 2), the hydroxamate occupies the binding site of the acetylated lysine side chain, the native substrates of the enzyme. Considering the CIP priority of the substituents, *R*-configured inhibitors with the described scaffold **6** mimic *S*-configured lysine derivatives.

In order to modify the linker, the aromatic moiety was changed to introduce another complexation site in form of a pyridine (**6h**) or a thiophene unit (**6i**) able to introduce a slightly bent structure. Apparently, introduction of an additional hydrogen bond acceptor or complexation site by replacing a phenyl by a pyridine ring leads to a reduced activity of the inhibitors. In conclusion, non-polar linker units are important for optimal interaction with the hydrophobic channel of histone deacetylases. As the inhibition of HDAC1 by compound **6h** was reduced manifold compared to HDAC6, this inhibitor is more selective for HCAC6. Interestingly, a slight modification of the angle of the rigid linker from 180° to 156° by replacing the phenyl ring by a thiophene ring (**6i**) enhances the inhibition significantly with good selectivity.

Docking studies of all compounds to available crystal structures of human HDAC1, 6 and 8 were performed to understand the observed in vitro inhibition data (see Experimental Section for details). As expected, the aromatic hydroxamate group of all inhibitors is coordinating the catalytic zinc ion and is hydrogen bonded to the conserved tyrosine and histidine residues as observed for the co-crystallized hydroxamates (e.g. Trichostatin A in HDAC6). The aromatic ring (phenyl, pyridine, or thiophene) is interacting with two conserved phenylalanines in the HDAC pocket (F150 and F205 in HDAC1, F620 and F680 in HDAC6, F152 and F208 in HDAC8).[40] The hydrophobic substituents in the propargylic position, which confer HDAC isoform selectivity, interact with residues located at the rim of the acetyl-lysine channel. The docking results for the most potent HDAC6 inhibitor **6i** showed that the benzofuran ring is interacting with the aromatic sidechains of W496 and H500 in the HDAC6 binding pocket whereas the cyclohexyl ring is located nearby the hydrophobic residues P501 and L749 (Figure 6). An additional hydrogen bond is observed between the amide of the capping group and S568. Due to the different angle of the rigid linker of compounds **6a-6h**, the hydrophobic capping group adopts a slightly different orientation whereas the benzofuran ring is interacting as observed for **6i**. In the case of the *S*-configured capping groups, the benzofuran ring is shifted away from W496 (Figure S1 Supporting Information). A significant correlation between the calculated docking scores (Glide SP) and the HDAC6 inhibitory activities was observed (r^2 = 0.82, RMSE = 0.13, q^2_{LOO} = 0.72, Figure S2 and Table S1, Supporting Information).

Docking into the HDAC1 crystal structure (PDB ID 4BKX) [41] gave the best docking score for the unsubstituted derivative **6d** (Figure 7 and Table S1, Supporting Information). The benzofuran ring of the capping group is interacting with the aromatic side chains of Y204, F205 as well as with the backbone of P206. The hydrophobic substitutions of the capping group (**6a-6c** and **6e-i)** showed a similar orientation in the HDAC1 binding pocket but with less favourable docking scores (Figure S3 and S4, Supporting Information) which might explain their decreased inhibitory activities. As observed for the HDAC6 inhibition values, a significant correlation with the calculated GlideSP score was obtained (r^2 = 0.71, RMSE = 0.24, q^2_{LOO} = 0.46, Figure S4 and Table S1, Supporting Information).

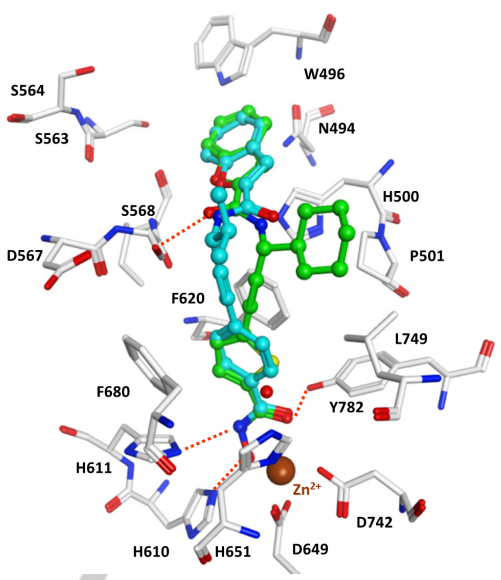

Figure 6. Binding mode of the most potent HDAC6 inhibitors **6i** (colored green) and **6e** (colored cyan) derived by the docking study. Hydrogen bonds between inhibitor and HDAC6 are shown as orange dashed lines. Water molecules are shown as red spheres.

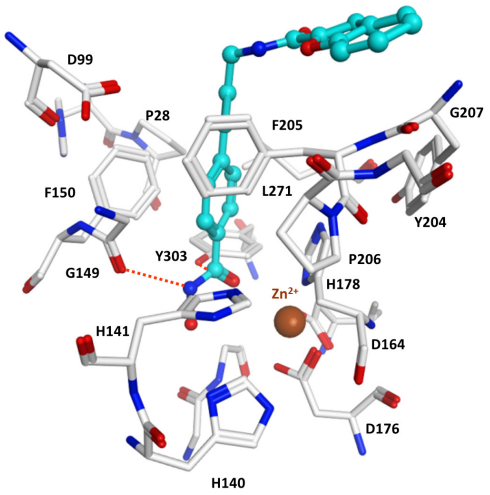

Figure 7. Binding mode of the most potent HDAC1 inhibitor **6d** (colored cyan) derived by the docking study. Hydrogen bonds between inhibitor and HDAC1 are shown as orange dashed lines.

The docking of the inhibitors into the HDAC8 binding pocket showed that the capping group is pointing out of the more open HDAC8 pocket resulting in fewer contacts between the capping group and the pocket residues (Figure S5, Supporting Information). The rigid propargyl linker does not allow interactions with the side pocket of HDAC8 that have been shown to be important for highly potent "linkerless" HDAC8 inhibitors.[42]

Cytotoxicity tests were performed with the cervix carcinoma cell line KB-3-1. The cytotoxicity of all investigated compounds correlates qualitatively with the affinity to HDAC1, but not at all with the affinity to HDAC6 which is in accordance to previous publications.[19,20] (Table 2). This observation confirms the previous study of Lagger et al. who elucidated the effect of HDAC1 inhibition by microarray analysis and knockout mice.[16] Interestingly, the thiophene based compound **6i** is much less cytotoxic, considering its activity to inhibit HDAC1. Decreased general cytotoxicity of HDAC6 selective compounds like **6h** or **6i** makes them potentially interesting for non-cancer indications, like neuroprotection.[43]

Conclusions

By coupling enantiomerically pure propargylamines to aromatic hydroxamate derivatives a versatile type of compounds has been obtained and used as a linker scaffold for potent HDAC inhibitors. *R*-configured propargylamines that mimic *S*-configured lysine based substrates display higher activity and selectivity towards HDAC6. In particular, thiophene derivative **6i** emerged as a selective low nM HDAC6 inhibitor with good HDAC selectivity while retaining low cytotoxicity. The observed structure-activity relationship data, in particular with respect to the influence of chirality, are clearly supported by molecular docking studies.

Experimental Section

A detailed description of the techniques, experiments, characterizations, spectra and chromatograms is given in the Supporting Information. Compounds **1-4** are described in the Supporting Information.

General procedure for the synthesis of propargylic aromatics **5**. The aromatic halide **2** or **3** (1.6 eq) was added to a solution of propargylamine **4a-g** (1 eq) in a mixture of dry THF and piperidine (3:1, 6 eq piperidine) and the solution was thoroughly degassed by freeze-pump-thaw cycles (3 x 10^{-2} mbar). Afterwards the catalysts $PdCl_2(PPh_3)_2$ (1 mol%) and CuI (2 mol%) were added and the solution warmed to rt. While the slightly yellow solution was stirred for 0.5 to 14 h at ambient temperature, a colourless precipitate formed. The suspension was diluted with saturated NH_4Cl solution (ca. 10 mL) and neutralized with aqueous HCl (2 M). After separation of the phases, the aqueous layer was extracted with Et_2O (3 x 20 mL) and the combined organic phases dried over Na_2SO_4. The crude product was purified by column chromatography (EtOAc/PE, 1:1) and the title compound isolated in form of a faint green oil.

Methyl 4-((*S*)-3-(((*S*)-*tert*-Butylsulfinyl)amino)-3-cyclohexylprop-1-yn-1-yl)benzoate (**5a**). Yield: 102.2 mg, 0.27 mmol, 66%. ^{1}H NMR (500 MHz, $CDCl_3$) δ = 7.93 (d, ^3J = 8.2 Hz, 2H, ar-2-**H**, ar-6-**H**), 7.47 (d, ^3J = 8.1 Hz, 2H, ar-3-**H**, ar-5-**H**), 4.06 (dd, ^3J = 7.5 Hz, ^3J = 5.8 Hz, 1H, HNC$^{\alpha}$**H**), 3.88 (s, 3H, CO_2CH_3), 3.36 (d, ^3J = 7.4 Hz, 1H, N**H**), 1.93-1.82 (m, 2H, cy-**H**), 1.83-1.72 (m, 2H, cy-**H**), 1.70-1.61 (m, 2H, cy-**H**), 1.22 (s, 9H, C(C**H**$_3$)$_3$), 1.19-1.06 (m, 5H, cy-**H**). ^{13}C NMR (126 MHz, $CDCl_3$) δ = 166.6 (**C**O_2), 131.8 (ar-**C**-2, ar-**C**-6), 129.6 (ar-**C**-3, ar-**C**-5), 129.4 (ar-**C**-4), 127.6 (ar-**C**-1), 91.4 (C$^{\alpha}$-C≡**C**-ar), 85.0 (C$^{\alpha}$-**C**≡C-ar), 56.5 (S**C**(CH$_3$)$_3$), 53.8 (CO_2**C**H$_3$), 52.3 (HN**C**$^{\alpha}$), 43.5 (cy-**C**-1), 29.7 (cy-**C**-2), 28.6 (cy-**C**-6), 26.4 (cy-**C**-4), 26.0 (cy-**C**-5), 25.9 (cy-**C**-3), 22.7 (C(**C**H$_3$)$_3$). $C_{21}H_{29}NO_3S$ (375.53 g mol^{-1})**.** MS (ESI): *m/z* = 398.1804 (calcd. 398.1760 [M+Na]$^+$). TLC: R_f (EtOAc/PE, 1:1) = 0.25.

Ethyl 4-((*S*)-3-(((*S*)-*tert*-Butylsulfinyl)amino)-5-methylhex-1-yn-1-yl)benzoate (**5b**). Instead of the methyl ester **2a**, ethyl 4-iodobenzoate was applied. Yield: 23.0 mg, 63.3 mmol, 94%. ^{1}H NMR (500 MHz, $CDCl_3$) δ = 7.94 (d, ^3J = 8.4 Hz, 2H, ar-2-**H**, ar-6-**H**), 7.47 (d, ^3J = 8.4 Hz, 2H, ar-3-**H**, ar-5-**H**), 4.35 (q, ^3J = 7.1 Hz, 2H, CO_2-C**H**$_2$), 4.27 (q, ^3J = 7.52 Hz, 1H, C$^{\alpha}$**H**), 3.36 (d, ^3J = 7.3 Hz, 1H, N**H**), 1.91 (m, 1H, Me_2C**H**), 1.67 (t, ^3J = 7.4 Hz, 2H, HNC$^{\alpha}$H-C**H**$_2$), 1.37 (t, ^3J = 7.13 Hz, 3H, CO_2CH_2C**H**$_3$), 1.22 (s, 9H, SC(C**H**$_3$)$_3$), 0.95 (d, ^3J = 6.7 Hz, 3H, MeCHC**H**$_3$), 0.95 (d, ^3J = 6.7 Hz, 3H, MeCHC**H**$_3$). ^{13}C NMR (126 MHz, $CDCl_3$) δ = 166.2 (**C**O_2Et), 131.7 (ar-**C**-3, ar-**C**-5), 130.0 (ar-**C**-1), 129.4 (ar-**C**-2, ar-**C**-6), 127.4 (ar-**C**-4), 92.4 (C$^{\alpha}$-**C**≡C-ar), 84.2 (C$^{\alpha}$-C≡**C**-ar), 61.2 (CO_2**C**H$_2$), 56.4 (**C**(CH$_3$)$_3$), 47.1 (NH**C**$^{\alpha}$), 46.2 (C$^{\alpha}$**C**H$_2$), 25.1 ((CH$_3$)$_2$**C**H), 22.6 (SC(**C**H$_3$)$_3$), 22.3 (CH(**C**H$_3$)$_2$), 14.4 (CO_2CH_2**C**H$_3$). $C_{20}H_{29}NO_3S$ (363.52 g mol^{-1}), MS (ESI): *m/z* = 386.17499 (calcd. 386.17604 [M+Na]$^+$). TLC: R_f (EtOAc/PE, 1:1) = 0.26.

Methyl 4-((*S*)-3-(((*S*)-*tert*-Butylsulfinyl)amino)-4-methylpent-1-yn-1-yl)benzoate (**5c**). Yield: 69.0 mg, 0.206 mmol, 83%. ^{1}H NMR (500 MHz, $CDCl_3$) δ = 7.93 (d, ^3J = 8.3 Hz, 2H, ar-2-**H**, ar-6-**H**), 7.46 (d, ^3J = 8.3 Hz, 2H, ar-3-**H**, ar-5-**H**), 4.09 (dd, ^3J = 7.0 Hz, ^3J = 5.2 Hz, 1H, HNC$^{\alpha}$**H**), 3.87 (s, 3H, CO_2CH_3), 3.41 (d, ^3J = 7.0 Hz, 1H, N**H**), 2.00 (m, 1H, (CH$_3$)$_2$C**H**), 1.22 (s, 9H, C(C**H**$_3$)$_3$), 1.04 (d, ^3J = 6.8 Hz, 3H, MeCHC**H**$_3$), 1.04 (d, ^3J = 6.8 Hz, 3H, MeCHC**H**$_3$). ^{13}C NMR (126 MHz, $CDCl_3$) δ = 166.6 (**C**O_2(CH$_3$)), 131.8 (ar-**C**-3), 129.6 (ar-**C**-1), 129.4 (ar-**C**-2), 127.5 (ar-**C**-4), 90.9 (C$^{\alpha}$-**C**≡C-ar), 85.0 (C$^{\alpha}$-C≡**C**-ar), 56.4 (**C**(CH$_3$)$_3$), 54.4 (HN**C**$^{\alpha}$), 52.3 (CO_2**C**H$_3$), 33.9 (**C**H(CH$_3$)$_2$), 22.7 (C(**C**H$_3$)$_3$), 19.1 (MeCH**C**H$_3$), 17.7 (MeCH**C**H$_3$). $C_{18}H_{25}NO_3S$ (335.46), MS (ESI): *m/z* = 358.1452 (calcd. 358.1447 [M+Na]$^+$), $[\alpha]_D^{20}$ = 13.7 (*c* = 0.325, $CHCl_3$). TLC: R_f (EtOAc/PE, 1:1) = 0.28. IR (ATR): $\tilde{\nu}$ [cm^{-1}] = 2958 (CH_3/CH_3), 2927-2873 (CH_3/CH_2), 1720 (CO_2Me), 1603 (N-H), 1280 (S=O), 1442/1306/1173 (ar, C=C), 770 (S-C).

Methyl 4-((*R*)-3-(((*R*)-*tert*-Butylsulfinyl)amino)-4-methylpent-1-yn-1-yl)benzoate (**5e**). Yield: 105.7 mg, 0.315 mmol, 64%. ^{1}H NMR (600 MHz, $CDCl_3$) δ = 7.96 (d, ^3J = 8.3 Hz, 2H, ar-2-**H**, ar-6-**H**), 7.50 (d, ^3J = 8.3 Hz, 2H, ar-3-**H**, ar-5-**H**), 4.13 (t, ^3J = 5.7 Hz, 1H, NH-C$^{\alpha}$**H**), 3.91 (s, 3H, CO_2C**H**$_3$), 3.38 (d, ^3J = 6.9 Hz, 1H, N**H**), 2.04 (dqq, ^3J = 6.6 Hz, ^3J = 6.7 Hz, ^3J = 6.7 Hz, 1H, (CH$_3$)$_2$C**H**), 1.26 (s, 9H, C(C**H**$_3$)$_3$), 1.07 (d, ^3J = 6.8 Hz, 3H, CHC**H**$_3$), 1.07 (d, ^3J = 6.7 Hz, 3H, CHC**H**$_3$). ^{13}C NMR (126 MHz, $CDCl_3$) δ = 166.6 (**C**O_2Me), 131.8 (ar-2-**C**, ar-6-**C**), 129.6 (ar-4-**C**), 129.4 (ar-3-**C**, ar-5-**C**), 127.5 (ar-1-**C**), 90.9 (C$^{\alpha}$-**C**≡C-ar), 85.0 (C$^{\alpha}$-C≡**C**-ar), 56.4 (S**C**(CH$_3$)$_3$), 54.4 (HNC$^{\alpha}$**H**), 52.3 (CO_2**C**H$_3$), 33.9 ((CH$_3$)$_2$**C**H), 22.7 (C(**C**H$_3$)$_3$), 19.1 ((CH$_3$)CH-**C**H$_3$), 17.7 ((CH$_3$)CH-**C**H$_3$). MS (ESI): *m/z* = 358.1452 (calcd. 358.1447 [M+Na]$^+$), TLC: R_f (EtOAc/PE, 1:1) = 0.28. IR (ATR): $\tilde{\nu}$ [cm^{-1}] = 2958 (CH_3/CH_3), 2927-2873 (CH_3/CH_2), 1720 (CO_2Me), 1603 (N-H), 1280 (S=O), 1442/1306/1173 (ar, C=C), 770 (S-C).

Ethyl 4-((*R*)-3-(((*R*)-*tert*-Butylsulfinyl)amino)-5-methylhex-1-yn-1-yl)benzoate (**5f**). Instead of the methyl ester **2a**, ethyl 4-iodobenzoate was applied. Yield: 671.3 mg, 1.847 mmol, 95%. ^{1}H NMR (500 MHz, $CDCl_3$) δ = 7.97 (d, ^3J = 8.3 Hz, 2H, ar-2-**H**, ar-6-**H**), 7.49 (d, ^3J = 8.4 Hz, 2H, ar-3-**H**, ar-5-**H**), 4.37 (q, ^3J = 7.1 Hz, 2H, CO_2C**H**$_2$), 4.29 (q, ^3J = 7.5 Hz, 1H, HNC$^{\alpha}$**H**), 3.39 (d, ^3J = 7.3 Hz, 1H, N**H**), 1.92 (m, 1H, (CH$_3$)$_2$C**H**), 1.70 (t, ^3J = 7.4 Hz, 2H, HNCH-C**H**$_2$), 1.39 (t, ^3J = 7.1 Hz, 3H, CO_2CH_2C**H**$_3$), 1.25 (s, 9H, C(C**H**$_3$)$_3$), 0.98 (d, ^3J = 6.7 Hz, 3H, (CH$_3$)CHC**H**$_3$), 0.98 (d, ^3J = 6.7 Hz, 3H, (CH$_3$)CHC**H**$_3$). ^{13}C NMR (126 MHz, $CDCl_3$) δ = 166.2 (**C**O_2Et), 131.7 (ar-**C**-2, ar-**C**-6), 130.0 (ar-**C**-1), 129.4 (ar-**C**-3, ar-**C**-5), 127.4 (ar-**C**-4), 92.4 (C$^{\alpha}$-**C**≡C-ar), 84.2 (C$^{\alpha}$-C≡**C**-ar), 61.2 (CO_2**C**H$_2$CH$_3$), 56.4 (**C**(CH$_3$)$_3$), 47.1 (**C**$^{\alpha}$NH), 46.2 (C$^{\alpha}$**C**H$_2$), 25.1 ((CH$_3$)$_2$**C**H), 22.6 (C(**C**H$_3$)$_3$), 22.3 (CH(**C**H$_3$)$_2$), 14.4 (CO_2CH_2**C**H$_3$). $C_{20}H_{29}NO_3S$ (363.52 g mol^{-1}), MS (ESI): *m/z* = 386.17645 (calcd. 386.17604 [M+Na]$^+$). TLC: R_f (EtOAc/PE, 1:1) = 0.26.

Methyl 4-((*R*)-3-(((*R*)-*tert*-Butylsulfinyl)amino)-3-cyclohexylprop-1-yn-1-yl)benzoate (**5g**). Yield: 114.8 mg, 0.306 mmol, 74%. ^{1}H NMR (500 MHz, $CDCl_3$) δ = 7.93 (d, ^3J = 8.2 Hz, 2H, ar-2-**H**, ar-6-**H**), 7.47 (d, ^3J = 8.1 Hz, 2H, ar-3-**H**, ar-5-**H**), 4.06 (dd, ^3J = 7.5 Hz, ^3J = 5.8 Hz, 1H, HNC$^{\alpha}$**H**), 3.88

(s, 3H, $CO_2C\mathbf{H_3}$), 3.36 (d, ^3J = 7.4 Hz, 1H, N**H**), 1.93-1.82 (m, 2H, cy-**H**), 1.83-1.72 (m, 2H, cy-**H**), 1.70-1.61 (m, 2H, cy-**H**), 1.22 (s, 9H, $C(C\mathbf{H_3})_3$), 1.19-1.06 (m, 5H, cy-**H**). ^{13}C NMR (126 MHz, $CDCl_3$) δ = 166.6 ($\mathbf{C}O_2$), 131.8 (ar-**C**-2, ar-**C**-6), 129.6 (ar-**C**-4), 129.4 (ar-**C**-3, ar-**C**-5), 127.6 (ar-**C**-1), 91.4 (C^{α}-**C**≡C-ar), 85.0 (C^{α}-C≡**C**-ar), 56.5 ($(CH_3)_3\mathbf{C}$), 53.8 ($CO_2\mathbf{C}H_3$), 52.3 (HN$\mathbf{C}^{\alpha}$H), 43.5 (HNCH$\mathbf{C}H_2$), 29.7 (cy-**C**-2), 28.6 (cy-**C**-6), 26.4 (cy-**C**-4), 26.0 (cy-**C**-5), 25.9 (cy-**C**-3), 22.7 ($C(\mathbf{C}H_3)_3$). $C_{21}H_{29}NO_3S$ (375.53 g mol^{-1}), MS (ESI): *m/z* = 398.1804 (calcd. 398.1760 $[M+Na]^+$). TLC: R_f (EtOAc/PE, 1:1) = 0.25.

Methyl 5-((*R*)-3-(((*R*)-*tert*-Butylsulfinyl)amino)-3-cyclohexylprop-1-yn-1-yl)picolinate (**5h**). Picolinate **2b** was used as aromatic halide. This reaction was performed at 60 °C for 16 h. Yield: 64.6 mg, 0.172 mmol, 41%. ^{1}H NMR (300 MHz, $CDCl_3$) δ = 8.71 (dd, ^4J = 2.1 Hz, ^5J = 0.9 Hz, 1H, py-6-**H**), 8.04 (dd, ^3J = 8.1 Hz, ^5J = 0.9 Hz, 1H, py-3-**H**), 7.86 (dd, ^3J = 8.1 Hz, ^4J = 2.1 Hz, 1H, py-4-**H**), 4.07 (dd, ^3J = 7.9 Hz, ^3J = 5.9 Hz, 1H, HNC^{α}**H**), 3.98 (s, 3H, $CO_2C\mathbf{H_3}$), 3.37 (d, ^3J = 7.9 Hz, 1H, N**H**), 1.94-1.83 (m, 3H, cy-**H**), 1.81-1.72 (m, 3H, cy-**H**), 1.71-1.62 (m, 2H, cy-**H**), 1.22 (s, 9H, $C(C\mathbf{H_3})_3$), 1.18-1.07 (m, 3H, cy-**H**). ^{13}C NMR (151 MHz, $CDCl_3$) δ = 165.3 ($\mathbf{C}O_2(CH_3)$), 152.1 (py-**C**-6), 146.3 (py-**C**-2), 139.9 (py-**C**-4), 124.5 (py-**C**-3), 123.5 (py-**C**-5), 95.1 (C^{α}-**C**≡C-ar), 82.0 (C^{α}-C≡**C**-ar), 56.7 ($\mathbf{C}(CH_3)_3$), 54.0 ($CO_2\mathbf{C}H_3$), 53.1 (NH$\mathbf{C}^{\alpha}$), 43.5 (cy-**C**-1), 29.6 (cy-**C**-2), 28.8 (cy-**C**-6), 26.3 (cy-**C**-4), 26.0 (cy-**C**-5), 25.9 (cy-**C**-3), 22.7 ($C(\mathbf{C}H_3)_3$). $C_{20}H_{28}N_2O_3S$ (376.51 g mol^{-1}), MS (ESI): *m/z* = 399.1625 (calcd. 399.1713 $[M+Na]^+$), IR (ATR): $\tilde{\nu}$ [cm^{-1}] = 2927 (CH_2), 2854 (CH_2, NH), 1724 (CO_2Me), 1448 (ar, C=C), 1302 (ar, C=C). TLC: R_f (EtOAc/PE, 1:2) = 0.05.

Methyl 5-((*R*)-3-(((*R*)-*tert*-Butylsulfinyl)amino)-3-cyclohexylprop-1-yn-1-yl)thiophene-2-carboxylate (**5i**). Thiophene derivative **2c** was applied as aromatic halide. Yield: 36.6 mg, 95.9 nmol, 23%. ^{1}H NMR (500 MHz, $CDCl_3$) δ = 7.62 (d, ^3J = 3.9 Hz, 1H, thiophene-2-**H**), 7.12 (d, ^3J = 3.9 Hz, 1H, thiophene-3-**H**), 4.06 (d, ^3J = 6.2 Hz, 1H, HNC^{α}**H**), 3.87 (s, 3H, $CO_2C\mathbf{H_3}$), 1.91-1.84 (m, 2H, cy-**H**), 1.83-1.74 (m, 2H, cy-**H**), 1.73-1.62 (m, 2H, cy-**H**), 1.29 (s, 9H, $C(C\mathbf{H_3})_3$), 1.26-1.02 (m, 5H, cy-**H**). ^{13}C NMR (126 MHz, $CDCl_3$) δ = 162.1 ($\mathbf{C}O_2(CH_3)$), 133.9 (thiophene-**C**-5), 133.3 (thiophene-**C**-3), 132.7 (thiophene-**C**-4), 129.1 (thiophene-**C**-1), 94.1 (C^{α}H**C**≡C-ar), 78.8 (C^{α}HC≡**C**-ar), 57.6 ($\mathbf{C}(CH_3)_3$), 55.1 ($CO_2\mathbf{C}H_3$), 52.5 (HN$\mathbf{C}^{\alpha}$H), 43.6 (cy-**C**-1), 29.6 (cy-**C**-2), 28.9 (cy-**C**-6), 26.3 (cy-**C**-4), 25.9 (cy-**C**-5), 25.8 (cy-**C**-3), 22.8 ($C(\mathbf{C}H_3)_3$). $C_{19}H_{27}NO_3S_2$ (381.55 g mol^{-1}). MS (ESI): *m/z* = 404.1298 (calcd. 404.1325 $[M+Na]^+$), $[\alpha]_D^{22}$ = -11.3 (*c* = 0.40, MeOH). TLC: R_f (EtOAc/PE, 1:1) = 0.16. IR (ATR): $\tilde{\nu}$ [cm^{-1}] = 2927 (cy, CH_2), 2844 (CH_3), 1711 (CO_2CH_3), 1448 (HNS=O), 1258 (ar, C=C), 1173 (ar, C=C), 1097 (ar, C=C).

General procedure for the preparation of hydroxamic acids **6** from **5**:

Acidic methanolysis of the Bus or Boc group: HCl (4 M in dioxane, 4 eq) was slowly added under vigorous stirring to a solution of **5** (1 eq) in methanol (20 mL). After 2-4 h, the solvent of the slightly yellow reaction mixture was evaporated to yield a yellow solid. This solid was treated with DCM and the solvent coevaporated (3 x). The ammonium chloride salt of the desired amine was isolated quantitatively in form of a colourless, odourless solid.

Acylation with benzofuran-2-carbonyl chloride: The propargylammonium chloride salt (65.0 mg, 0.24 mmol, 1.0 eq) and benzofuran-2-carbonyl chloride (1.1 eq) were dissolved in THF (1.5 mL) at -30 °C under inert gas atmosphere. Triethylamine (2.5 eq) was added and the mixture was slowly warmed up to room temperature. Afterwards the mixture was diluted with ethyl acetate (10 mL) and washed with hydrochloric acid (0.5 M, 10 mL), sodium bicarbonate solution (10 mL) and brine (10 mL). The organic layer was dried over sodium sulfate, the solvent evaporated and the crude product was purified by column chromatography (EtOAc/Petrolether, 1:1) to yield carboxamide as a colorless, crystalline solid (20-45%).

Hydroxamate formation: Hydroxylamine (0.5 mL, 50% in H_2O) was added dropwise to a vigorously stirred solution of ester (1 eq) in a mixture of THF and MeOH (1:1, 4 mL). Aqueous NaOH (1 M, ca. 4 drops) was added until a pH value of 10-11 was reached and the reaction mixture was stirred further 14 h at ambient temperature. After neutralization of the solution with aqueous HCl (1 M, 6-8 drops) and addition of Et_2O (ca. 10 mL), the hydroxamic acids precipitated in form of a colourless solid. The solvent was evaporated under reduced pressure and the remainder was dissolved in acetonitrile (1 mL) and the inhibitors **6** were purified by preparative RP-HPLC in form of a colourless solid.

(*S*)-*N*-(1-Cyclohexyl-3-(4-(hydroxaminocarbonyl)phenyl)prop-2-yn-1-yl)benzofuran-2-carboxamide (**6a**). Yield: 25.9 mg, 62 µmol, 24%. ^{1}H NMR (600 MHz, CD_3OD) δ = 11.29 (s, 1H, CONHO**H**), 9.18 (d, ^3J = 8.5 Hz, 1H, benzofuran-CON**H**OH), 7.77 (d, ^3J = 8.4 Hz, 1H, benzofuran-8-**H**), 7.73 (d, ^3J = 8.4 Hz, 2H, ar-2-**H**, ar-6-**H**), 7.67 (t, ^3J = 8.4 Hz, 1H, benzofuran-5-**H**), 7.54 (d, ^4J = 0.7 Hz, 1H, benzofuran-3-**H**), 7.52 (d, ^3J = 8.3 Hz, 2H, ar-3-**H**, ar-5-**H**), 7.47 (dd, ^3J = 6.8 Hz, ^3J = 7.2 Hz, 1H, benzofuran-7-**H**), 7.34 (t, ^3J = 7.5 Hz, 1H, benzofuran-6-**H**), 4.86 (d, ^3J = 7.9 Hz, 1H, HNC^{α}**H**), 2.04 (m, 1H, cy-**H**), 1.86-1.67 (m, 3H, cy-**H**), 1.61 (m, 1H, cy-**H**), 1.29-1.11 (m, 5H, cy-**H**), 1.05 (m, 1H, cy-**H**). ^{13}C NMR (151 MHz, DMSO) δ = 163.5 (**C**ONHOH), 157.7 (**C**ONHC$^{\alpha}$), 154.4 (benzofuran -**C**-9), 148.6 (benzofuran-**C**-2), 132.5 (ar-**C**-4), 131.5 (ar-**C**-1), 127.3 (ar-**C**-3, ar-**C**-5), 127.1 (ar-**C**-2, ar-**C**-6), 127.1 (ar-**C**-4), 125.1 (benzofuran-**C**-7), 123.8 (benzofuran-**C**-6), 122.9 (benzofuran-**C**-5), 112.0 (benzofuran-**C**-8), 110.2 (benzofuran-**C**-3), 90.7 (C^{α}-**C**≡C-ar), 82.4 (C^{α}-C≡**C**-ar), 46.3 ($\mathbf{C}^{\alpha}$), 41.7 (cy-**C**-1), 29.3 (cy-**C**-2), 29.2 (cy-**C**-6), 25.9 (cy-**C**-4), 25.4 (cy-**C**-5), 25.4 (cy-**C**-3). $C_{25}H_{24}N_2O_4$ (417.47 gmo^{-1}). MS (nanoESI): *m/z* = 439.16283 (calc. 439.1638 $[M+Na]^+$). $[\alpha]_D^{20}$ = 58.3 (*c* = 0.105, MeOH). IR (ATR): $\tilde{\nu}$ [cm^{-1}] = 3224 (CONH*O*-H), 2920 (N-HCO), 2851 (CON-HOH), 1730 (HO-NH-C=O), 1632 (NH-C=O), 1591 (C_{ar}=C_{ar}), 1581 (C_{ar}=C_{ar}), 1502 (C_{ar}=C_{ar}), 1445 (C_{ar}=C_{ar}).

(*S*)-*N*-(1-(4-(Hydroxaminocarbonyl)phenyl)-5-methylhex-1-yn-3-yl)benzofuran-2-carboxamide (**6b**). Yield: 10.88 mg, 27.87 µmol, 43%. ^{1}H NMR (600 MHz, CD_3OD) δ = 7.74 (t, ^3J = 5.2 Hz, 1H, benzofuran-8-**H**), 7.72 (d, ^3J = 8.4 Hz, 2H, ar-6-***H***, ar-2-**H**), 7.62 (d, ^3J = 8.4 Hz, 1H, benzofuran-5-**H**), 7.55 (s, 1H, benzofuran-3-**H**), 7.52 (d, ^3J = 8.3 Hz, 2H, ar-5-**H**, ar-3-**H**), 7.47 (t, ^3J = 7.8 Hz, 1H, benzofuran-6-**H**), 7.33 (t, ^3J = 7.5 Hz, 1H, benzofuran-7-**H**), 5.23 (t, ^3J = 7.7 Hz, 1H, HNC^{α}**H**), 1.88 (m, 1H, $(H_3C)_2C\mathbf{H}$), 1.84 (t, ^3J = 6.9 Hz, 2H, $C\mathbf{H_2}$), 1.04 (d, ^3J = 6.5 Hz, 3H, $C\mathbf{H_3}$), 1.04 (d, ^3J = 6.5 Hz, 3H, $C\mathbf{H_3}$). ^{13}C NMR (151 MHz, CD_3OD) δ = 167.3 (ar-**C**ONHOH), 160.3 (benzofuran-**C**ONH), 156.5 (benzofuran-**C**-9), 149.6 (benzofuran-**C**-2), 133.2 (ar-**C**-1), 132.8 (ar-**C**-3, ar-**C**-5), 128.7 (benzofuran-**C**-6), 128.3 (ar-**C**-4), 128.2 (ar-**C**-2, ar-**C**-6), 127.6 (benzofuran-**C**-4), 124.9 (benzofuran-**C**-7), 123.8 (benzofuran-**C**-8), 112.9 (benzofuran-**C**-5), 111.8 (benzofuran-**C**-3), 91.9 (C^{α}-**C**≡C-ar), 82.8 (C^{α}-C≡**C**-ar), 45.4 (HN$\mathbf{C}^{\alpha}$H), 41.2 ($\mathbf{C}H_2$), 26.4 ($(CH_3)_2\mathbf{C}H$), 22.8 ($\mathbf{C}H_3$), 22.5 ($\mathbf{C}H_3$). $C_{23}H_{22}N_2O_4$ (390.44 g mol^{-1}), MS (nanoESI): *m/z* = 391.1623 (calc. 391.1652 $[M+H]^+$). $[\alpha]_D^{22}$ = 26.3 (*c* = 0.065, MeOH). IR (ATR): $\tilde{\nu}$ [cm^{-1}] = 3237 (CONHOH), 2955 (N-HCO), 2924 (CH_3), 2867 (CON-HOH), 1644 (C=ONHOH), 1597 (NHC=O), 1521-1505 (C_{ar}=C_{ar}).

(*S*)-*N*-(1-(4-(Hydroxaminocarbonyl)phenyl)-4-methylpent-1-yn-3-yl)benzofuran-2-carboxamide (**6c**). Yield: 19.1 mg, 50.7 µmol, 16%. ^{1}H NMR (600 MHz, CD_3OD): δ = 7.73 (d, ^3J = 8.4 Hz, 1H, benzofuran-8-**H**), 7.72 (d, ^3J = 8.4 Hz, 2H, ar-2-**H**, ar-6-**H**), 7.62 (d, ^3J = 8.4 Hz, 1H, benzofuran-5-**H**), 7.56 (s, 1H, benzofuran-3-**H**), 7.54 (d, ^3J = 8.3 Hz, 2H, ar-3-**H**, ar-5-**H**), 7.47 (t, ^3J = 8.2 Hz, 1H, benzofuran-6-**H**), 7.33 (t, ^3J = 7.5 Hz, 1H, benzofuran-7-**H**), 4.97 (d, ^3J = 7.3 Hz, 1H, C^{α}**H**), 2.17 (dqq, ^3J = 6.3 Hz, ^3J = 6.7 Hz, ^3J = 6.7 Hz, 1H, $(CH_3)_2C\mathbf{H}$), 1.19 (d, ^3J = 6.7 Hz, 3H, $C\mathbf{H_3}$), 1.11 (d, ^3J = 6.7 Hz, 3H, $C\mathbf{H_3}$). ^{13}C NMR (151 MHz, CD_3OD): δ = 165.9 (**C**ONHOH), 159.1 (benzofuran-**C**ONH), 155.1 (benzofuran-**C**-9), 148.2 (benzofuran-**C**-2), 131.8 (ar-**C**-1), 131.4 (ar-**C**-3, ar-**C**-5), 127.3 (benzofuran-**C**-4), 126.9 (ar-**C**-4), 126.8 (ar-**C**-2, ar-**C**-6), 126.2 (benzofuran-**C**-6), 123.5 (benzofuran-**C**-7), 122.4 (benzofuran-**C**-8), 111.5 (benzofuran-**C**-5), 110.4 (benzofuran-**C**-3), 89.2 (C^{α}-**C**≡C-ar), 82.6 (C^{α}-C≡**C**-ar), 47.8 ($\mathbf{C}^{\alpha}$), 33.2 ($(CH_3)_2\mathbf{H}$**C**), 18.2 ($\mathbf{C}H_3$), 17.8 ($\mathbf{C}H_3$). $C_{22}H_{20}N_2O_4$ (376.41 g mol^{-1}. MS (nanoESI): *m/z* = 377.1516 (calcd. 377.1496 $[M+H]^+$). $[\alpha]_D^{22}$ = 58.9 (*c* = 0.425, MeOH), IR (ATR): $\tilde{\nu}$ [cm^{-1}] = 3231 (CONHO-H), 2962 (N-HCO), 2930 (CH_3), 2870 (CON-HOH), 1641 (C=ONHOH), 1597 (NHC=O), 1423 (C_{ar}=C_{ar}).

(*R*)-*N*-(1-(4-(Hydroxaminocarbonyl)phenyl)-4-methylpent-1-yn-3-yl)benzofuran-2-carboxamide (**6e**). Yield: 15.2 mg, 40.4 µmol, 37%. ^{1}H NMR (600 MHz, CD_3OD): δ = 7.71 (d, ^3J = 8.4 Hz, 1H, benzofuran-8-**H**), 7.71 (d, ^3J = 8.4 Hz, 2H, ar-2-**H**, ar-6-**H**), 7.60 (d, ^3J = 8.4 Hz, 1H, benzofuran-5-**H**), 7.53 (s, 1H, benzofuran-3-**H**), 7.52 (d, ^3J = 8.3 Hz, 2H, ar-3-**H**, ar-5-**H**), 7.45 (td, ^3J = 7.9 Hz, ^4J = 1.3 Hz, 1H, benzofuran-6-**H**), 7.31 (t, ^3J = 7.5 Hz, 1H, benzofuran-7-**H**), 4.95 (d, ^3J = 7.3 Hz, 1H, NHC$^\alpha$**H**), 2.16 (m, 1H, $(CH_3)_2$C**H**), 1.17 (d, ^3J = 6.7 Hz, 3H, C**H$_3$**), 1.09 (d, ^3J = 6.7 Hz, 3H, C**H$_3$**). ^{13}C NMR (151 MHz, CD_3OD): δ = 165.8 (**C**ONHOH), 159.1 (benzofuran-**C**ONH), 155.1 (benzofuran-**C**-9), 148.2 (benzofuran-**C**-2), 131.8 (ar-**C**-1), 131.4 (ar-**C**-3), 127.3 (benzofuran-**C**-4), 126.9 (ar-**C**-4), 126.8 (ar-**C**-2, ar-**C**-6), 126.2 (benzofuran-**C**-6), 123.5 (benzofuran-**C**-7), 122.4 (benzofuran-**C**-8), 111.5 (benzofuran-**C**-5), 110.4 (benzofuran-**C**-3), 89.2 (C$^\alpha$-**C**≡C-ar), 82.6 (C$^\alpha$-C≡**C**-ar), 47.8 (NH**C**$^\alpha$), 33.2 ($(CH_3)_2$H**C**), 18.2 (**C**H$_3$), 17.8 (**C**H$_3$). $C_{22}H_{20}N_2O_4$ (376.41 mol^{-1}). MS (nanoESI): *m*/*z* = 399.1347 (calcd. 399.1315 [M+Na]$^+$). $[\alpha]_D^{22}$ = -61.4 (*c* = 0.355, MeOH). IR (ATR): $\tilde{\nu}$ [cm^{-1}] = 3231 (CONHO-H), 2962 (N-HCO), 2930 (CH_3), 2870 (CON-HOH), 1641 (C=ONHOH), 1597 (NHC=O), 1423 (C_{ar}=C_{ar}).

(*R*)-*N*-(1-(4-(Hydroxaminocarbonyl)phenyl)-5-methylhex-1-yn-3-yl)benzofuran-2-carboxamide (**6f**). Yield: 5.48 mg, 14.0 µmol, 9%. ^{1}H NMR (600 MHz, CD_3OD): δ = 7.71 (d, ^3J = 7.2 Hz, 1H, benzofuran-8-**H**), 7.68 (d, ^3J = 8.3 Hz, 2H, ar-6-**H**, ar-2-**H**), 7.58 (d, ^3J = 8.2 Hz, 1H, benzofuran-5-**H**), 7.51 (s, 1H, benzofuran-3-**H**), 7.49 (d, ^3J = 7.9 Hz, 2H, ar-5-**H**, ar-3-**H**), 7.44 (t, ^3J = 7.6 Hz, 1H, benzofuran-6-**H**), 7.29 (t, ^3J = 7.3 Hz, 1H, benzofuran-7-**H**), 5.19 (t, ^3J = 7.6 Hz, 1H, NHC$^\alpha$**H**), 1.89 (m, 1H, $(CH_3)_2$C**H**), 1.79 (t, ^3J = 7.2 Hz, 2H, C$^\alpha$C**H$_2$**), 1.00 (d, ^3J = 6.3 Hz, 6H, C(C**H$_3$**)$_2$). ^{13}C NMR (151 MHz, CD_3OD): δ = 165.9 (**C**ONHOH), 158.9 (benzofuran-**C**ONH), 155.1 (benzofuran-**C**-9), 148.2 (benzofuran-**C**-2), 131.8 (ar-**C**-1), 131.4 (ar-**C**-3, ar-**C**-5), 127.3 (benzofuran-**C**-6), 126.9 (ar-**C**-4), 126.8 (ar-**C**-2, ar-**C**-6), 126.2 (benzofuran-**C**-4), 123.5 (benzofuran-**C**-7), 122.4 (benzofuran-**C**-8), 111.5 (benzofuran-**C**-5), 110.4 (benzofuran-**C**-3), 90.5 (C$^\alpha$H**C**≡C-ar), 81.4 (C$^\alpha$HC≡**C**-ar), 44.0 (NH**C**$^\alpha$H), 39.8 (C$^\alpha$**C**H$_2$), 25.0 ($(CH_3)_2$**C**H), 21.4 (**C**H$_3$), 21.2 (**C**H$_3$). $C_{23}H_{22}N_2O_4$ (390.44 g mol^{-1}). MS (nanoESI): *m*/*z* = 391.1623 (calcd. 391.1652 [M+H]$^+$). $[\alpha]_D^{22}$ = -34.2 (*c* = 0.1, MeOH). IR (ATR): $\tilde{\nu}$ [cm^{-1}] = 3237 (CONHO-H), 2955 (N-HCO), 2924 (CH_3), 2867 (CON-HOH), 1644 (C=ONHOH), 1597 (NHC=O), 1521, 1505 (C_{ar}=C_{ar}).

(*R*)-*N*-(1-Cyclohexyl-3-(4-(hydroxaminocarbonyl)phenyl)prop-2-yn-1-yl)-benzofuran-2-carboxamide (**6g**). Yield: 4.8 mg, 12 µmol, 6%. ^{1}H NMR (600 MHz, CD_3OD) δ = 7.74 (d, ^3J = 8.1 Hz, 1H, benzofuran-8-**H**), 7.72 (d, ^3J = 8.5 Hz, 2H, ar-**C**-2, ar-**C**-6), 7.62 (d, ^3J = 8.4 Hz, 1H, benzofuran-5-**H**), 7.54 (s, 1H, benzofuran-3-**H**), 7.53 (d, ^3J = 8.4 Hz, 2H, ar-**C**-3, ar-**C**-5), 7.46 (ddd, ^3J = 8.4 Hz, ^3J = 7.1 Hz, ^4J = 1.3 Hz, 1H, benzofuran-7-**H**), 7.33 (t, ^3J = 7.5 Hz, 1H, benzofuran-6-**H**), 4.96 (d, ^3J = 7.9 Hz, 1H, NHC$^\alpha$**H**), 2.12 (m, 1H, cy-**H**), 1.92 (m, 1H, cy-**H**), 1.89-1.77 (m, 3H, cy-**H**), 1.71 (m, 1H, cy-**H**), 1.41-1.13 (m, 5H, cy-**H**). ^{13}C NMR (151 MHz, CD_3OD) δ = 163.5 (**C**ONHOH), 157.7 (**C**ONHC), 154.4 (benzofuran-**C**-9), 148.6 (benzofuran-**C**-2), 132.5 (ar-**C**-1), 131.5 (ar-**C**-2, ar-**C**-6), 127.3 (ar-**C**-3, ar-**C**-5), 127.1 (benzofuran-**C**-4), 127.1 (ar-**C**-4), 125.1 (benzofuran-**C**-7), 123.8 (benzofuran-**C**-6), 122.9 (benzofuran-**C**-5), 112.0 (benzofuran-**C**-8), 110.2 (benzofuran-**C**-3), 90.7 (C$^\alpha$-**C**≡C-ar), 82.4 (C$^\alpha$-C≡**C**-ar), 46.3 (**C**$^\alpha$), 41.7 (cy-**C**-1), 29.3 (cy-**C**-2), 29.2 (cy-**C**-6), 25.9 (cy-**C**-4), 25.4 (cy-**C**-5), 25.4 (cy-**C**-3). $C_{25}H_{24}N_2O_4$ (416.48 g mol^{-1}). MS (nanoESI): *m*/*z* = 439.1639 (calcd. 439.1628 [M+Na]$^+$). $[\alpha]_D^{22}$ = -55.8 (*c* = 0.069, MeOH). IR (ATR): $\tilde{\nu}$ [cm^{-1}] = 3224 (CONHO-H), 2920 (N-HCO), 2851 (CON-HOH), 1730 (HO-NH-C=O), 1632 (NH-C=O), 1591 (C_{ar}=C_{ar}), 1581 (C_{ar}=C_{ar}), 1502 (C_{ar}=C_{ar}), 1445 (C_{ar}=C_{ar}).

(*R*)-*N*-(1-Cyclohexyl-3-(2-(hydroxaminocarbonyl)pyridin-5-yl)prop-2-yn-1-yl)benzofuran-2-carboxamide (**6h**). Yield: 9.99 mg, 23.9 µmol, 25%. ^{1}H NMR (500 MHz, CD_3OD) δ = 8.63 (s, 1H, py-6-**H**), 8.01 (m, 1H, py-4-**H**), 7.97 (m, 1H, py-3-**H**), 7.73 (d, ^3J = 7.7 Hz, 1H, benzofuran-8-**H**), 7.61 (d, ^3J = 8.4 Hz, 1H, benzofuran-5-**H**), 7.55 (s, 1H, benzofuran-3-**H**), 7.46 (t, ^3J = 7.7 Hz, 1H, benzofuran-6-**H**), 7.32 (t, ^3J = 7.5 Hz, 1H, benzofuran-7-**H**), 4.99 (d, ^3J = 8.0 Hz, 1H, C$^\alpha$**H**), 3.35 (s, 1H, CONHO**H**), 2.12 (d, ^2J = 12.3 Hz, 1H, cy-1-**H**), 1.92 (d, ^2J = 12.5 Hz, 1H, cy-4-**H**), 1.89-1.77 (m, 3H, cy-**H**), 1.70 (d, ^2J = 11.9 Hz, 1H, cy-4-**H**), 1.40-1.10 (m, 5H, cy-**H**). ^{13}C NMR (126 MHz, CD_3OD) δ = 163.5 (**C**ONHOH), 160.5 (**C**ONH), 156.5 (benzofuran-**C**-9), 152.2 (py-**C**-2), 149.5 (py-**C**-6), 149.4 (benzofuran-**C**-2), 141.1 (py-**C**-3), 128.7 (benzofuran-**C**-4), 128.4 (benzofuran-**C**-6), 125.0 (py-**C**-5), 124.1 (benzofuran-**C**-7), 123.8 (benzofuran-**C**-8), 122.6 (py-**C**-4), 112.9 (benzofuran-**C**-5), 111.9 (benzofuran-**C**-3), 94.3 (C$^\alpha$-**C**≡C-ar), 81.1 (C$^\alpha$-C≡**C**-ar), 48.2 (NH**C**$^\alpha$), 43.7 (cy-**C**-1), 30.7 (cy-**C**-2), 30.7 (cy-**C**-6), 27.3 (cy-**C**-4), 26.9 (cy-**C**-5), 26.9 (cy-**C**-3). $C_{24}H_{23}N_3O_4$ (417.47 g mol^{-1}). MS (nanoESI): *m*/*z* = 440.1574 (calcd. 440.1581 [M+Na]$^+$). $[\alpha]_D^{22}$ = -56.7 (*c* = 0.07, MeOH), IR (ATR): $\tilde{\nu}$ [cm^{-1}] = 3262 (CONHO-H), 2926 (N-HCO), 2850 (CON-HOH), 2359 (C≡C), 2341 (C≡C), 1648 (NH-C=O), 1594 (C_{ar}=C_{ar}), 1553 (C_{ar}=C_{ar}), 1505 (C_{ar}=C_{ar}), 1448 (C_{ar}=C_{ar}).

(*R*)-*N*-(1-Cyclohexyl-3-(5-(hydroxaminocarbonyl)thiophen-2-yl)prop-2-yn-1-yl)benzofuran-2-carboxamide (**6i**). Yield: 5.92 mg, 14 µmol, 16%. ^{1}H NMR (300 MHz, DMSO-d_6) δ = 11.34 (s, 1H, CON**H**OH), 9.23 (d, ^3J = 8.6 Hz, 1H, CON**H**), 7.78 (dd, ^3J = 7.8 Hz, ^4J = 1.3 Hz, 1H, benzofuran-8-**H**), 7.69 (d, ^3J = 7.9 Hz, 1H, benzofuran-5-**H**), 7.66 (s, 1H, benzofuran-3-**H**), 7.52 (d, 1H, thiophen-3-**H**), 7.48 (ddd, ^3J = 8.5 Hz, ^3J = 7.4 Hz, ^4J = 1.4 Hz, 1H, benzofuran-6-**H**), 7.35 (td, ^3J = 7.7 Hz, ^4J = 0.7 Hz, 1H, benzofuran-7-**H**), 7.31 (d, 1H, ^3J = 4.0 Hz, thiophen-4-**H**), 4.88 (t, ^3J = 8.4 Hz, 1H, NHC$^\alpha$**H**), 3.47 (s, 1H, CONHO**H**), 1.99 (m, 1H, cy-1-**H**), 1.89-1.68 (m, 4H, cy-**H**), 1.62 (d, ^2J = 9.0 Hz, 1H, cy-4-**H**), 1.30-1.10 (m, 4H, cy-**H**), 1.02 (m, 1H, cy-**H**). ^{13}C NMR (126 MHz, DMSO-d_6) δ = 158.4 (**C**ONHOH), 157.6 (**C**ONH), 154.3 (benzofuran-**C**-9), 148.4 (benzofuran-**C**-2), 138.3 (thiophene-**C**-3), 133.1 (thiophene-**C**-4), 127.5 (benzofuran-**C**-6), 127.1 (thiophene-**C**-2), 127.0 (benzofuran-**C**-4), 125.3 (benzofuran-**C**-6), 123.8 (benzofuran-**C**-7), 122.9 (benzofuran-**C**-8), 111.9 (benzofuran-**C**-5), 110.1 (benzofuran-**C**-3), 99.5 (thiophene-**C**-5), 94.7 (C$^\alpha$-**C**≡C-ar), 75.7 (C$^\alpha$-C≡**C**-ar), 46.3 (NH**C**$^\alpha$), 41.5 (cy-**C**-1), 29.2 (cy-**C**-2), 29.1 (cy-**C**-6), 25.8 (cy-**C**-4), 25.3 (cy-**C**-5), 25.3 (cy-**C**-3). $C_{23}H_{22}N_2O_4S$ (422.50). MS (nanoESI): *m*/*z* = 445.1190 (calcd. 445.1193 [M+Na]$^+$). $[\alpha]_D^{22}$ = -25.7 (*c* = 0.07, MeOH). IR (ATR): $\tilde{\nu}$ [cm^{-1}] = 3227 (CONHO-H), 2924 (N-HCO), 2851 (CON-HOH), 2357 (C≡C), 2341 (C≡C), 1730 (OHNH-C=O), 1648 (NH-C=O), 1594 (C_{ar}=C_{ar}), 1515 (C_{ar}=C_{ar}), 1448 (C_{ar}=C_{ar}).

In vitro testing [36–38]

OptiPlate-96 black microplates (Perkin Elmer) were used. Assay volume was 60 µL. 52 µL of human recombinant HDAC1 (BPS Bioscience, Catalog #: 50051) or human recombinant HDAC6 (BPS Bioscience, Catalog #: 50006) in incubation buffer (50 mM Tris-HCl, pH 8.0, 137 mM NaCl, 2.7 mM KCl, 1 mM $MgCl_2$ and 1 mg/mL BSA) were incubated with 3 µL of different concentrations of inhibitors in DMSO and 5 µL of the fluorogenic substrate ZMAL (Z-(Ac)Lys-AMC) [44] (126 µM) for 90 min at 37 °C. After the incubation time 60 µL of the stop solution, comprising 33 µM Trichostatin A (TSA) and 6 mg/mL trypsin in trypsin buffer (Tris-HCl 50 mM, pH 8.0, NaCl 100 mM), were added. The plate was incubated again at 37 °C for 30 min and fluorescence was measured on a BMG LABTECH POLARstar OPTIMA plate reader (BMG Labtechnologies, Germany) with an excitation wavelength of 390 nm and an emission wavelength of 460 nm.

Inhibition of human HDAC8 was measured in ½ AREAPLATE-96 F microplates (Perkin Elmer) with an assay volume of 30 µL. HDAC8 enzyme was obtained as described before.[45] 22.5 µL of enzyme in incubation buffer (50 mM KH_2PO_4, 15 mM Tris, pH 7.5, 3 mM $MgSO_4$*7 H_2O, 10 mM $MgSO_4$) were mixed with 2.5 µL of inhibitor in DMSO and 5 µL of Z-L-Lys(ε-trifluoroacetyl)-AMC (150 µM). The plate was incubated at 37 °C for 90 min. 30 µL of the stop solution (see HDAC1 and HDAC6) were added and the plate was incubated again at 37 °C for 30 min. Measurement was performed as described for HDAC1/6.

Cytotoxicity assays

The cytotoxicity of the inhibitors was tested as previously described.[39] The KB-3-1 cells were cultivated as a monolayer in DMEM (Dulbecco's modified Eagle medium) with glucose (4.5 g L^{-1}), L-glutamine, sodium pyruvate and phenol red, supplemented with 10% fetal bovine serum (FBS). The cells were maintained at 37 °C and 5.3% CO_2-humidified air. On the day before the test, the cells (70% confluence) were detached with trypsin-ethylenediamine tetraacetic acid (EDTA) solution (0.05%; 0.02% in DPBS) and placed in sterile 96-well plates in a density of 10 000 cells in 100 µL medium per well. The dilution series of the compounds were prepared from stock solutions in DMSO of concentrations of 1 mM or 10 mM. The stock solutions were diluted with culture medium at least 50 times. Some culture medium was added to the wells to adjust the volume of the wells to the wanted dilution factor. The dilution prepared from stock solution was added to the wells. Each concentration was tested in six replicates. Dilution series were prepared by pipetting liquid from well to well. The control contained the same concentration of DMSO as the first dilution. After incubation for 72 h at 37 °C and 5.3% CO_2-humidified air, 30 µL of an aqueous resazurin solution (175 µM) was added to each well. The cells were incubated at the same conditions for 6 h. Subsequently, the fluorescence was measured. The excitation was effected at a wavelength of 530 nm, whereas the emission was recorded at a wavelength of 588 nm. The EC_{50} values as the drug concentrations resulting in 50% cell viability were calculated as a sigmoidal dose response curve using GRAPHPAD PRISM 4.03.

Docking studies

The resolved crystal structure of human HDACs complexed with inhibitors were taken from the Protein Data Bank (PDB, www.rcsb.org) [46]: HDAC6 complexed with TSA (PDB ID 5EDU, resolution 2.79 Å) [25], HDAC8 complexed with Trapoxin A (PDB ID 5VI6, resolution 1.24 Å) [40] and HDAC1 complexed with acetate (PDB ID 4BKX, resolution 3.0 Å). [41] All protein structures were prepared using Schrödinger's Protein Preparation Wizard [47] by adding hydrogen atoms, assigning protonation states and minimizing the protein. All inhibitors were prepared for docking using the LigPrep tool [48] as implemented in Schrödinger's software, where all possible tautomeric forms as well as stereoisomers were generated and energy minimized using the OPLS force field. Conformers of the prepared inhibitor structures were calculated with ConfGen using the default settings and allowing minimization of the output conformations. Inhibitor docking was performed using the program Glide [49] in the Standard Precision mode. In HDAC6 and HDAC8, the conserved water molecule bound to His180 (HDAC8, His651 in HDAC6) was considered during the docking procedure. The chosen docking protocol could perfectly reproduce the co-crystallized inhibitors in HDAC1, HDAC6 and HDAC8 as demonstrated in former studies.[50–52] Top ranked HDAC-inhibitor complexes were visually analyzed in MOE2012.10.[53]

Acknowledgements

Financial support by Deutsche Forschungsgemeinschaft (SE609/10-1, JU295/13-1, and SI846/13-1) is gratefully acknowledged.

Conflict of interest

The authors declare no conflict of interest.

Keywords: cancer | heterocycle | inhibitor | propargylamine | histone deacetylase

References

[1] M. Dokmanovic, C. Clarke, P. A. Marks, *Mol. Cancer Res. MCR* **2007**, *5*, 981-989.
[2] J. M. Greer, P. A. McCombe, *Biol. Targets Ther.* **2012**, *6*, 307-327.
[3] C. Cook, T. F. Gendron, K. Scheffel, Y. Carlomagno, J. Dunmore, M. DeTure, L. Petrucelli, *Hum. Mol. Genet.* **2012**, *21*, 2936-2945.
[4] G. I. Aldana-Masangkay, K. M. Sakamoto, *J. Biomed. Biotechnol.* **2011**, *2011*, 875824.
[5] Y.-S. Lee, K.-H. Lim, X. Guo, Y. Kawaguchi, Y. Gao, T. Barrientos, P. Ordentlich, X.-F. Wang, C. M. Counter, T.-P. Yao, *Cancer Res.* **2008**, *68*, 7561-7569.
[6] A. A. Lane, B. A. Chabner, *J. Clin. Oncol. Off. J. Am. Soc. Clin. Oncol.* **2009**, *27*, 5459-5468.
[7] B. S. Mann, J. R. Johnson, M. H. Cohen, R. Justice, R. Pazdur, *The Oncologist* **2007**, *12*, 1247-1252.
[8] T. Vanhaecke, P. Papeleu, G. Elaut, V. Rogiers, *Curr. Med. Chem.* **2004**, *11*, 1629-1643.
[9] J. A. Plumb, P. W. Finn, R. J. Williams, M. J. Bandara, M. R. Romero, C. J. Watkins, N. B. La Thangue, R. Brown, *Mol. Cancer Ther.* **2003**, *2*, 721-728.
[10] J. Arts, P. Angibaud, W. Floren, B. Janssen, P. King, J. van Dun, L. Janssen, T. Geerts, R. W. Tuman, D. L. Johnson, L. Andries, M. Jung, M. Janicot, K. van Emelen, *Br. J. Cancer* **2007**, *97*, 1344-1353.
[11] Y. B. Kim, K. H. Lee, K. Sugita, M. Yoshida, S. Horinouchi, *Oncogene* **1999**, *18*, 2461-2470.
[12] K. V. Butler, J. Kalin, C. Brochier, G. Vistoli, B. Langley, A. P. Kozikowski, *J. Am. Chem. Soc.* **2010**, *132*, 10842-10846.
[13] H. Ueda, H. Nakajima, Y. Hori, T. Fujita, M. Nishimura, T. Goto, M. Okuhara, *J. Antibiot. (Tokyo)* **1994**, *47*, 301-310.
[14] W. K. Kelly, O. A. O'Connor, L. M. Krug, J. H. Chiao, M. Heaney, T. Curley, B. MacGregore-Cortelli, W. Tong, J. P. Secrist, L. Schwartz, S. Richardson, E. Chu, S. Olgac, P. A. Marks, H. Scher, V. Richon, *J. Clin. Oncol. Off. J. Am. Soc. Clin. Oncol.* **2005**, *23*, 3923-3931.
[15] Z.-Q. Ning, Z.-B. Li, M. J. Newman, S. Shan, X.-H. Wang, D.-S. Pan, J. Zhang, M. Dong, X. Du, X.-P. Lu, *Cancer Chemother. Pharmacol.* **2012**, *69*, 901-909.
[16] G. Lagger, D. O'Carroll, M. Rembold, H. Khier, J. Tischler, G. Weitzer, B. Schuettengruber, C. Hauser, R. Brunmeir, T. Jenuwein, C. Seiser, *EMBO J.* **2002**, *21*, 2672-2681.
[17] C. M. Trivedi, Y. Luo, Z. Yin, M. Zhang, W. Zhu, T. Wang, T. Floss, M. Goettlicher, P. R. Noppinger, W. Wurst, V. Ferrari, C. Abrams, P. J. Gruber, J. Epstein, *Nat. Med.* **2007**, *13*, 324-331.
[18] C. L. Zhang, T. A. McKinsey, S. Chang, C. L. Antos, J. A. Hill, E. N. Olson, *Cell* **2002**, *110*, 479-488.
[19] S. J. Haggarty, K. M. Koeller, J. C. Wong, C. M. Grozinger, S. L. Schreiber, *Proc. Natl. Acad. Sci. U. S. A.* **2003**, *100*, 4389-4394.
[20] Y. Zhang, S. Kwon, T. Yamaguchi, F. Cubizolles, S. Rousseaux, M. Kneissel, C. Cao, N. Li, H.-L. Cheng, K. Chua, D. Lombard, A. Mizeracki, G. Matthias, F. Alt, S. Kochbin, P. Matthias, *Mol. Cell. Biol.* **2008**, *28*, 1688-1701.
[21] Y. Zhang, N. Li, C. Caron, G. Matthias, D. Hess, S. Khochbin, P. Matthias, *EMBO J.* **2003**, *22*, 1168-1179.
[22] S. Dallavalle, C. Pisano, F. Zunino, *Biochem. Pharmacol.* **2012**, *84*, 756-765.
[23] J. P. Dompierre, J. D. Godin, B. C. Charrin, F. P. Cordelières, S. J. King, S. Humbert, F. Saudou, *J. Neurosci. Off. J. Soc. Neurosci.* **2007**, *27*, 3571-3583.
[24] E. Hahnen, J. Hauke, C. Tränkle, I. Y. Eyüpoglu, B. Wirth, I. Blümcke, *Expert Opin. Investig. Drugs* **2008**, *17*, 169-184.
[25] Y. Hai, D. W. Christianson, *Nat. Chem. Biol.* **2016**, *12*, 741-747.
[26] M. S. Finnin, J. R. Donigian, A. Cohen, V. M. Richon, R. A. Rifkind, P. A. Marks, R. Breslow, N. P. Pavletich, *Nature* **1999**, *401*, 188-193.
[27] J. R. Somoza, R. J. Skene, B. A. Katz, C. Mol, J. D. Ho, A. J. Jennings, C. Luong, A. Arvai, J. J. Buggy, E. Chi, J. Tang, B.-C. Sang, E. Verner, R. Wynands, E. M. Leahy, D. Dougan, G. Snell, M. Navre, M. W. Knuth, R. Swans, D. McRee, L. W. Tari, *Structure* **2004**, *12*, 1325-1334.
[28] A. Schuetz, J. Min, A. Allali-Hassani, M. Schapira, M. Shuen, P. Loppnau, R. Mazitschek, N. P. Kwiatkowski, T. A. Lewis, R. L. Maglathin, T. McLean, A. Bochkarev, A. Plotnikov, M. Vedadi, C. Arrowsmith, *J. Biol. Chem.* **2008**, *283*, 11355-11363.
[29] Y. Liu, L. Li, J. Min, *Nat. Chem. Biol.* **2016**, *12*, 660-661.
[30] K. V. Butler, A. P. Kozikowski, *Curr. Pharm. Des.* **2008**, *14*, 505-528.
[31] T. Suzuki, *Chem. Pharm. Bull. (Tokyo)* **2009**, *57*, 897-906.
[32] M. Sendzik, *Acetylene Derivatives as Inhibitors of Histone Deacetylase*, **2006**, EP1656348 A1.
[33] H. C. Kolb, M. G. Finn, K. B. Sharpless, *Angew. Chem. Int. Ed Engl.* **2001**, *40*, 2004-2021.
[34] M. Wünsch, D. Schröder, T. Fröhr, L. Teichmann, S. Hedwig, N. Janson, C. Belu, J. Simon, S. Heidemeyer, P. Holtkamp, J. Rudlof, L. Klemme, A. Hinzmann, B. Neumann, H.-G. Stammler, N. Sewald, *Beilstein J. Org. Chem.* **2017**, in press.
[35] D. A. Cogan, G. Liu, J. Ellman, *Tetrahedron* **1999**, *55*, 8883-8904.

[36] D. Wegener, F. Wirsching, D. Riester, A. Schwienhorst, *Chem. Biol.* **2003**, *10*, 61-68.
[37] D. Wegener, C. Hildmann, D. Riester, A. Schwienhorst, *Anal. Biochem.* **2003**, *321*, 202-208.
[38] B. Heltweg, J. Trapp, M. Jung, *Methods San Diego Calif* **2005**, *36*, 332-337.
[39] B. Sammet, T. Bogner, M. Nahrwold, C. Weiss, N. Sewald, *J. Org. Chem.* **2010**, *75*, 6953-6960.
[40] N. J. Porter, D. W. Christianson, *ACS Chem. Biol.* **2017**, *12*, 2281-2286.
[41] P. J. Watson, C. J. Millard, A. M. Riley, N. S. Robertson, L. C. Wright, H. Y. Godage, S. M. Cowley, A. G. Jamieson, B. V. L. Potter, J. W. R. Schwabe, *Nat. Commun.* **2016**, *7*, 1-13.
[42] A. A. Tabackman, R. Frankson, E. S. Marsan, K. Perry, K. E. Cole, *J. Struct. Biol.* **2016**, *195*, 373-378.
[43] X. Xu, A. P. Kozikowski, L. Pozzo-Miller, *Front. Cell. Neurosci.* **2014**, *8*, 68.
[44] B. Heltweg, F. Dequiedt, E. Verdin, M. Jung, *Anal. Biochem.* **2003**, *319*, 42-48.
[45] M. Marek, S. Kannan, A.-T. Hauser, M. M. Mourão, S. Caby, V. Cura, D. A. Stolfa, K. Schmidtkunz, J. Lancelot, L. Andrade, J. P. Renaud, G. Oliveira, W. Sippl, M. Jung, J. Cavarelli, R. Pierce, C. Romier, *PLOS Pathog.* **2013**, *9*, 1-15.
[46] H. M. Berman, J. Westbrook, Z. Feng, G. Gilliland, T. N. Bhat, H. Weissig, I. N. Shindyalov, P. E. Bourne, *Nucleic Acids Res.* **2000**, *28*, 235-242.
[47] Schrödinger Release 2014-2: Schrödinger Suite 2014-2 Protein Preparation Wizard; Epik version 2.8, Schrödinger, LLC, New York, NY, **2014**; Impact version 6.3, Schrödinger, LLC, New York, NY, **2014**; Prime version 3.6, Schrödinger, LLC, New York, NY, **2014**.
[48] Schrödinger Release 2014-2: LigPrep, Schrödinger, LLC, New York, NY, **2014**.
[49] Small-Molecule Drug Discovery Suite 2014-2: Glide, version 9.8, Schrödinger, LLC, New York, NY, **2014**.
[50] S. Vojacek, K. Beese, Z. Alhalabi, S. Swyter, A. Bodtke, C. Schulzke, M. Jung, W. Sippl, A. Link, *Arch. Pharm. (Weinheim)* **2017**, *350*, 1-19.
[51] T. Heimburg, A. Chakrabarti, J. Lancelot, M. Marek, J. Melesina, A.-T. Hauser, T. B. Shaik, S. Duclaud, D. Robaa, F. Erdmann, M. Schmidt, C. Romier, R. Pierce, M. Jung, W. Sippl, *J. Med. Chem.* **2016**, *59*, 2423-2435.
[52] J. Senger, J. Melesina, M. Marek, C. Romier, I. Oehme, O. Witt, W. Sippl, M. Jung, *J. Med. Chem.* **2016**, *59*, 1545-1555.
[53] Molecular Operating Environment (MOE), 2014.09; Chemical Computing Group Inc., 1010 Sherbooke St. West, Suite #910, Montreal, QC, Canada, H3A 2R7, **2014**.

Entry for the Table of Contents

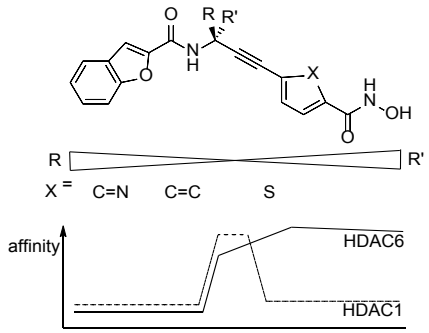

Chirality and angle matter: *R*-configured propargyl amides and a thiophene linker inducing a slight kink in the linker moiety provide inhibitors of HDAC6 with significantly increased affinity, selectivity and reduced cytotoxicity.